Two-source emission of nuclear fragments and conditional moments in nuclear fragmentation

Fu-hu Liu*
Department of Physics, Shanxi Teachers University, Linfen, Shanxi Province 041004, China

Yuri A. Panebratsev†
Laboratory of High Energies, Joint Institute for Nuclear Research, Dubna, Moscow Region 141980, Russia
(Received 30 March 1998)

A two-source emission picture is used to study the conditional moments of the charge distributions of projectile fragments in sulphur fragmentation at 200 GeV/nucleon by the Monte Carlo partition method. The distributions of the conditional moments are investigated and the logarithmic correlations between the conditional moments are found. The comparison of results of nuclear diffractive excitation, electromagnetic dissociation, and the Monte Carlo method are made. The calculated results are shown to be in agreement with the available experimental data. [S0556-2813(99)02402-4]

PACS number(s): 25.75.−q, 25.70.Mn, 25.70.Pq

I. INTRODUCTION

Nuclear fragmentation (hot-nuclei multifragmentation) in relativistic nucleus-nucleus collisions is an important experimental phenomenon [1]. According to the participant-spectator model [2,3], the interaction system in relativistic nucleus-nucleus collisions can be divided into three parts: a projectile spectator, a participant, and a target spectator in accordance with their relative velocity in the laboratory reference frame. The participant includes nucleons in the overlap volume of two nuclei coming into a violent collision and produces many mesons, nucleons, photons, lepton pairs, etc. The spectators include all other nucleons outside the overlap volume in a collision; they are broken up into nucleons and nuclear fragments. In order to study the nuclear reaction mechanism, it is necessary for us to study general characters of nuclear fragmentation (hot-nuclei multifragmentation) in relativistic nucleus-nucleus collisions [1].

Campi [4] has introduced the critical behavior method [5,6] in the study of hot-nuclei multifragmentation. He regards the hot-nuclei multifragmentation as a critical phenomenon and identifies the single-event moment (called the conditional moment) as follows:

$$M_k^j = \sum_{d \neq d_{\max}} d^k n^j(d), \tag{1}$$

where k is the moment order, $n^j(d) = 0,1,2,\ldots$, is the number of fragments of charge d appearing in the event j. The sum includes all the fragments, excluding the charge $d_{\max}$ of the heaviest one produced in the event. Campi has also introduced the normalized moment

$$S_k^j = M_k^j / M_1^j \tag{2}$$

which analyzes the charge distribution of fragments in 1 GeV/nucleon ^{197}Au-Em interactions [7]. Thus, he has obtained linear correlations between $\ln S_3$ and $\ln S_2$, as well as $\ln S_5$ and $\ln S_2$.

The situation for the correlation behavior, as discussed in Ref. [8], is not affected by omitting the limited condition $d \neq d_{\max}$ in formula (1). We have included the heaviest fragment in the following version of formula (1):

$$M_k^j = \sum_{d=1}^{d_{\max}} d^k n^j(d). \tag{3}$$

According to Eqs. (2) and (3), the correlations between $\ln S_3$ and $\ln S_2$, as well as $\ln S_5$ and $\ln S_2$ for 1 GeV/nucleon ^{197}Au-Em, 3.7 and 14.5 GeV/nucleon ^{28}Si-Em, 3.7 and 200 GeV/nucleon ^{16}O-Em and 200 GeV/nucleon ^{32}S-Em interactions, were obtained in Refs. [8–10]. The logarithmic correlations between the conditional moments were found. Meanwhile, the correlation behavior reveals a similarity for different incident energies, projectile sizes, and reaction mechanisms.

As it was shown in Refs. [8–10] the event distribution regions in the $\ln S_3$-$\ln S_2$ or $\ln S_5$-$\ln S_2$ planes for different incident nuclei are different. The correlations between the conditional moments and total charge, excluding the fragments with $d=1$ for 10.6 GeV/nucleon ^{197}Au-Em and 160 GeV/nucleon ^{208}Pb-Em interactions, were analyzed in Ref. [11]. The conditional moments in the diffractive excitation and electromagnetic dissociation of sulphur nuclei at 200 GeV/nucleon [12,13] based on a single emission source picture were studied by the Monte Carlo [8] partition method [14] in our previous work [15]. It is shown that the calculated results by the single emission source cannot present the experimental data of the conditional moment correlation and distribution in the case of excluding the heaviest fragment. To include the heaviest fragment, the calculated result can present only the experimental conditional moment correlation and cannot present perfectly the experimental conditional moment distribution. This means that more than one source is necessary to describe the conditional moment correlation and distribution in the nuclear fragmentation.

*Electronic address: liu@sunhe.jinr.ru; liufh@dns.sjstc.edu.cn; Now at the Laboratory of High Energies, JINR, Dubna, Moscow Region 141980, Russia.
†Electronic address: panebrat@sunhe.jinr.ru

In this paper, we study the conditional moment correlation and distribution in the diffractive excitation (DE) and electromagnetic dissociation (EMD) of sulphur nuclei at 200 GeV/nucleon by the Monte Carlo (MC) partition method based on a two-source emission picture and compare the calculated results with the experimental data of Refs. [12] and [13].

The paper is organized as follows. The descriptions of DE, EMD, and MC processes in the framework of two source emission method is given in Sec. II. Calculation results and comparison with available experimental data are presented in Sec. III. Discussion and conclusions are summarized in Sec. IV.

II. DESCRIPTIONS OF DE, EMD, AND MC PROCESSES

Up to now, three kinds of interactions in high-energy nucleus-nucleus collisions were found in experiment. They are nuclear reaction, electromagnetic dissociation, and elastic collision. Some of nuclear reaction events are diffractive excitation.

According to the discussions in Refs. [12] and [13], potential DE events are those interactions showing no visible target excitation (the number of target fragments is zero) when the interactions are examined in the emulsion using optical microscopes. Let θ_i denote the emission angle of the ith charged shower particle in an event; the DE event obeys the constraint condition of $\Sigma_i \sin\theta_i < 0.4$. Events with charged shower particles of $\sin\theta_i > 0.4$ are classified as non-DE ones. EMD events are generated in collisions involving large enough impact parameters so that no nuclear interactions occur. Extremely strong electromagnetic fields from heavy nuclei are produced for a very short time on the projectile; such events typically consist of projectile fragments, which proceed essentially in the direction of the projectile nucleus. The fragmentation cone was defined by $\theta < \theta_c = P_f / P_{\text{beam}}$, where P_f and P_{beam} are the Fermi momentum (estimated to be 200 MeV/c) and projectile momentum. The EMDs were then picked up using the criterion that the total charge of projectile fragments inside this cone is the charge of the projectile nucleus.

In the DE process, due to the existence of a relative motion between the participant and the spectator, the friction is assumed to be caused on the contact layer. Both the participant and the spectator obtain the heat of friction. It takes some time when the contact layer transmits the heat of friction to the other part of the spectator. This could not lead the whole spectator to an equilibrium state but could lead the contact layer and the other part to local equilibrium. Then, the contact layer and the other part of the spectator emit nuclear fragments with two different temperatures. In the EMD process, the local region of the colliding nucleus obtained the virtual photon energies from the collisions. Then, the local region has some excitation energy and remains in a high excitation state. A small part of the excitation energy of the local region is transmitted to the other part of the colliding nucleus. Then, the other part remains in a low excitation state. The whole colliding nucleus does not remain in the equilibrium state, but the local region obtained virtual photon energies, and the other part of the colliding nucleus remains in the local equilibrium states, respectively.

For the DE process, the contact layer and the other part of the projectile spectator are two different emission sources. For the EMD process, the two sources are the nuclear local region obtaining virtual photon energies and the other part, respectively. Obviously, the hot source is the contact layer or the local region obtaining virtual photon energies, and the cold source is the other part.

The MC method used in this paper is based on the following consideration. In collisions, the hot source is completely fragmented due to its high excitation. The cold source is partly fragmented with a given probability. In a collision, we assume that the hot source has charge Q, and the cold source has charge $Z-Q$, where Z is the charge of the projectile nucleus. Let F denote the probability of $Q=1$. Then, the probability of $Q=2$ is assumed to be F^2, the probability of $Q=3$ is F^3, etc. In all collisions, the normalized condition of probability can be written as

$$F + F^2 + \cdots + F^Q + \cdots + F^{Q_{\max}} = 1, \tag{4}$$

where $Q_{\max}$ is a maximum charge of the hot source in all collisions. Similarly, in the case of fragmentation of the cold source in a collision, the probability f of the cold source emitting one charge obeys

$$f + f^2 + \cdots + f^q + \cdots + f^{Z-Q} = 1, \tag{5}$$

where f^q $(q=1,2,\ldots,Z-Q)$ is the probability of the cold source emitting charge q in a collision.

The hot and cold sources emit charges Q and q, respectively. For a given Q or q, there are various possible configurations of charged fragments. For the hot source, it is completely fragmented. And for the cold source, it is partly fragmented with a given probability. The residual charge $Z-Q-q$ of the cold source is the charge of the residual nucleus in a collision. If the cold source is not fragmented in a collision, i.e., $q=0$, the charge of the residual nucleus is $Z-Q$. One of various possible configurations of Q, one of various possible configurations of q, and the residual nucleus with charge $Z-Q-q$ consist of a final state configuration. Let $n(d)$ denote the number of projectile fragments with charge d. A set $\{n(d)\}$ of all $n(d)$ in a probable fragmentation marks a final state configuration. Then, the set $\{n(d)\}$ is the sum of three kinds of fragments emitted from the hot and cold sources and the residual nucleus in the cold source, respectively.

Following the partition method [14] various possible configurations of a given charge can be obtained. For example, if the charge number is 5, there are seven kinds of possible configurations. Using fragment symbols, they are B, H+Be, He+Li, 2H+Li, H+2He, 3H+He, and 5H, respectively. In the case of charge numbers 1, 2, 3,...,15, the possible configuration numbers are 1, 2, 3, 5, 7, 11, 15, 22, 29, 40, 56, 77, 101, 134, and 176, respectively. The value of $Q_{\max}$, in our MC simulation, is taken to be 4. It is due to a maximum volume of the contact layer about one fourth of the projectile [16]. Then, $Q_{\max}=4$ for the ^{32}S projectile. The probability of fragmentation of the cold source is assumed to be 0.5. It reflects a low excitation energy obtained by the source, where the value 0.5 can be regarded as a fitting result to the

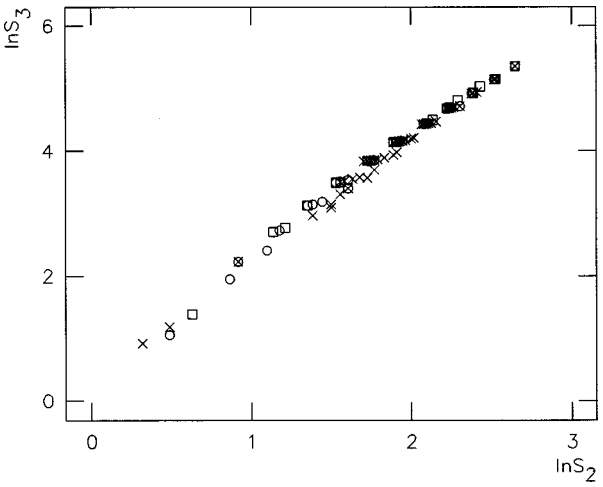

FIG. 1. Correlations between $\ln S_3$ and $\ln S_2$ in ^{32}S fragmentation at 200 GeV/nucleon in the case of including the heaviest fragment. Circles, squares, and crosses correspond to DE, EMD, and MC events, respectively.

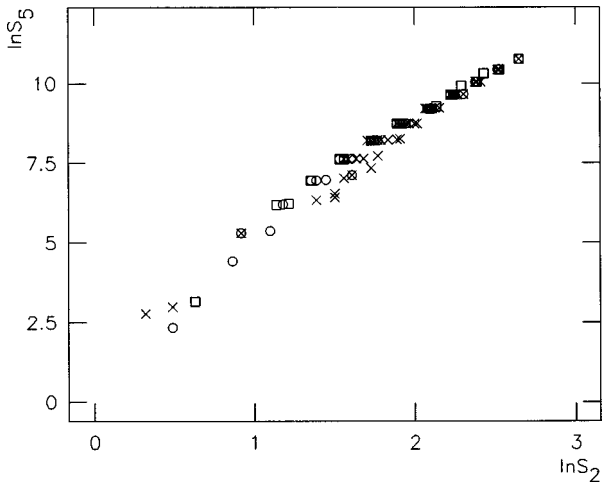

FIG. 3. As for Fig. 1, but showing a correlation between $\ln S_5$ and $\ln S_2$.

experimental data. The probabilities of various possible configurations for given charge are assumed to be $1/N$, where N is the number of possible configurations for given charge Q or q.

III. RESULTS

The normalized moments of sulphur nuclei fragmentation at 200 GeV/nucleon are calculated event by event in this paper. The fragmentation channel data obtained in Refs. [12] and [13] were used.

Figures 1 and 2 show the correlations between $\ln S_3$ and $\ln S_2$ calculated by formulas (2), (3) and (1), (2), respectively. The circles, squares, and crosses correspond to experimental DE and EMD events and MC simulated events. The event numbers are 191, 258, and 1000 correspond to the experimental DE and EMD processes and the MC simulation process based on a two-source emission picture, respectively. We would like to emphasize that there are some points in Figs. 1 and 2 corresponding to more than one event. It takes place in the case of including the heaviest fragment. Possible ranges of the values of $\ln S_2$ and $\ln S_3$ for the ^{32}S fragmentation process are $[0,4\ln 2]$ and $[0,8\ln 2]$, respectively.

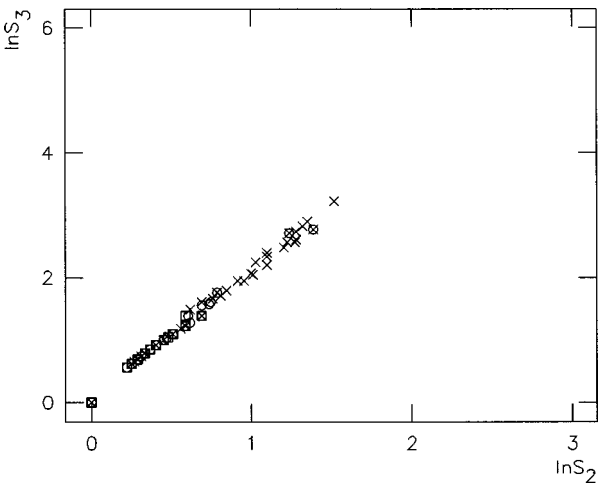

FIG. 2. As for Fig. 1, but excluding the heaviest fragment.

Figures 1 and 2 demonstrate the logarithmic correlations between the conditional moments in the cases of including and excluding the heaviest fragment, respectively. The equations of the correlation lines for DE, EMD, and MC events in Figs. 1 and 2 are as follows:

$$\ln S_3=(0.555\pm 0.025)+(1.823\pm 0.010)\ln S_2, \quad (6)$$

$$\ln S_3=(0.762\pm 0.022)+(1.741\pm 0.009)\ln S_2, \quad (7)$$

$$\ln S_3=(0.750\pm 0.011)+(1.746\pm 0.005)\ln S_2 \quad (8)$$

and

$$\ln S_3=(0.008\pm 0.004)+(2.080\pm 0.010)\ln S_2, \quad (9)$$

$$\ln S_3=(0.007\pm 0.003)+(2.028\pm 0.007)\ln S_2, \quad (10)$$

$$\ln S_3=(0.008\pm 0.002)+(2.069\pm 0.003)\ln S_2. \quad (11)$$

The value of calculated slope parameter is similar to the two slopes of the experimental correlation lines. The distribution region of simulated events in the $\ln S_3$-$\ln S_2$ plane is similar to that of DE and EMD events. There is no obvious difference between DE, EMD, and MC events. The obtained results both for the cases of including and excluding the heaviest fragment are in agreement with the experimental data.

The correlation between $\ln S_5$ and $\ln S_2$ calculated by formulas (2), (3) and (1), (2) are shown in Figs. 3 and 4, respectively. The circles, squares, and crosses correspond to experimental DE and EMD events and MC simulated events, respectively. In the case of including the heaviest fragment, a possible range of the values of $\ln S_5$ is $[0,16\ln 2]$ for the ^{32}S fragmentation process. The equations of the correlation lines for DE, EMD, and MC events in Fig. 3 are

$$\ln S_5=(2.134\pm 0.084)+(3.293\pm 0.035)\ln S_2, \quad (12)$$

$$\ln S_5=(2.809\pm 0.071)+(3.028\pm 0.028)\ln S_2, \quad (13)$$

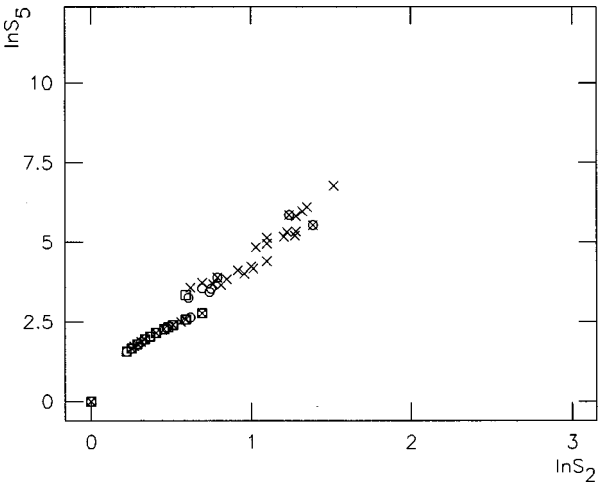

FIG. 4. As for Fig. 2, but showing a correlation between $\ln S_5$ and $\ln S_2$.

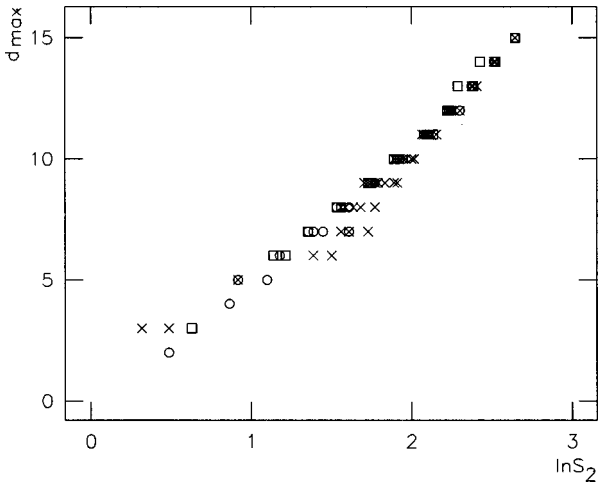

FIG. 5. Correlations between $d_{\max}$ and $\ln S_2$ in ^{32}S fragmentation at 200 GeV/nucleon in the case of including the heaviest fragment. Circles, squares, and crosses correspond to DE, EMD, and MC events, respectively.

and

$$\ln S_5 = (2.763 \pm 0.030) + (3.043 \pm 0.013) \ln S_2, \quad (14)$$

respectively. The equations of the correlation lines for DE, EMD, and MC events in Fig. 4 are

$$\ln S_5 = (0.044 \pm 0.019) + (4.361 \pm 0.048) \ln S_2, \quad (15)$$

$$\ln S_5 = (0.034 \pm 0.013) + (4.131 \pm 0.033) \ln S_2, \quad (16)$$

and

$$\ln S_5 = (0.044 \pm 0.007) + (4.289 \pm 0.015) \ln S_2, \quad (17)$$

respectively.

One can see from Figs. 3 and 4 that the correlations between $\ln S_5$ and $\ln S_2$ are similar to those between $\ln S_3$ and $\ln S_2$ in Figs. 1 and 2. The conclusions of Figs. 1 and 2 can be drawn from Figs. 3 and 4, as well. The results obtained in the framework in the two-source emission picture are in agreement with the experimental data.

Figures 1 and 3 show that DE and EMD events are very similar, if not equal. It is known that the DE and EMD processes are different in interaction mechanisms. The DE process is a nuclear reaction, and the EMD process is an electromagnetic interaction. The similar results show that the same fragmentation channel can be obtained by different interaction mechanisms, and the excited nuclei do not remember their history of formation.

Under the comparison $\ln S_3$ and $\ln S_5$ at the same $\ln S_2$ in Figs. 1–4, we found the exact linear correlations between the logarithmic conditional moments with different moment orders. The results support the applicability of the two-source emission picture in presenting the experimental data.

In order to compare theory and experiment in detail, Figs. 5 and 6 present the correlations between the heaviest fragment charge $d_{\max}$ and $\ln S_2$ for including and excluding the heaviest fragment in formula (2), respectively. The circles, squares, and crosses correspond to experimental DE and EMD events and MC simulated events, respectively. We do not care about the type of correlation between $d_{\max}$ and $\ln S_2$, but we care about the comparison between the calculated results and the experimental data. Figures 5 and 6 show similar results for three kinds of events. This means that the excited nuclei both from the DE and EMD processes do not remember their history of formation.

The $\ln S_2$ distributions, $P(\ln S_2)$, in the case of including and excluding the heaviest fragment are given in Figs. 7 and 8, respectively. The distribution is normalized to a 0.25 bin width of $\ln S_2$. The dashed, dotted, and solid histograms correspond to experimental DE and EMD events and MC simulated events, respectively. The $\ln S_2$ distributions for MC events in the case of including and excluding the heaviest fragment are similar to those of DE and EMD events. The experimental data can be presented by the calculated results based on a two-source emission picture.

If we condsider, as mentioned in Sec. I, the excited projectile nucleus as just one emission source, the calculated results cannot present experimental data of the conditional moment correlation (CMC) and distribution (CMD) in the case of excluding the heaviest fragment [15].

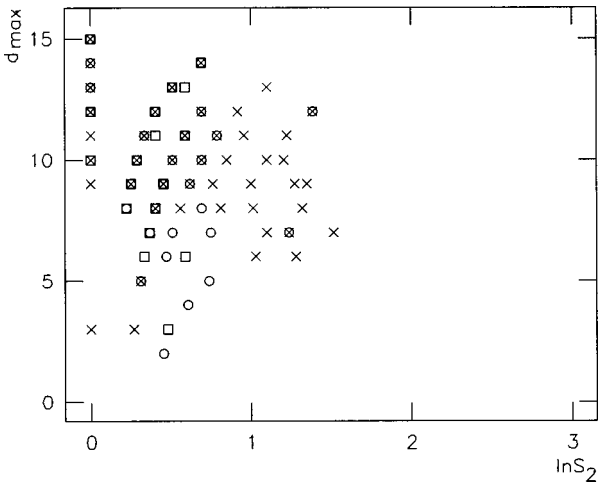

FIG. 6. As for Fig. 5, but excluding the heaviest fragment.

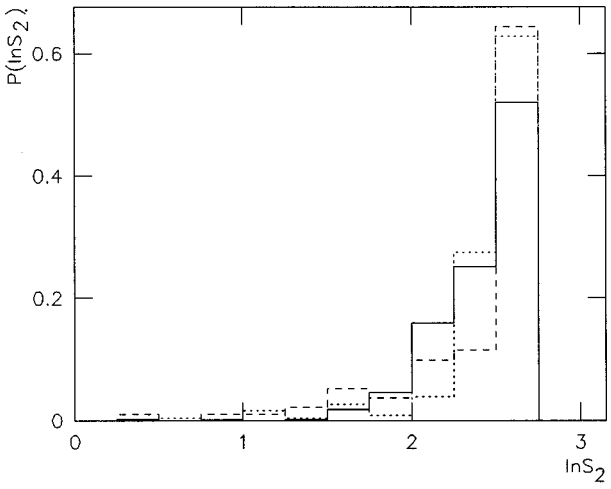

FIG. 7. The $\ln S_2$ distributions in ^{32}S fragmentation at 200 GeV/nucleon. The heaviest fragment is included. Dashed, dotted, and solid histograms correspond to DE, EMD, and MC events, respectively.

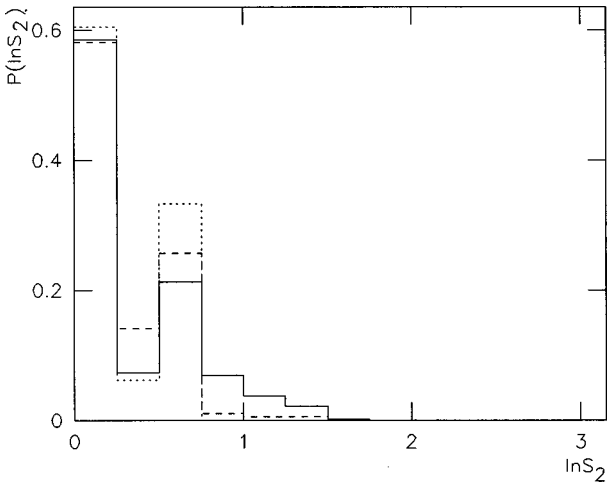

FIG. 8. As for Fig. 7, but excluding the heaviest fragment.

For including the heaviest fragment, the calculated result can present only the experimental CMC and cannot present the experimental CMD [15]. Here, we can see that the calculated results based on a two-source emission picture can present the experimental CMC and CMD, as well as the correlation between the heaviest fragment and the conditional moment, in the case of including and excluding the heaviest fragment.

IV. DISCUSSIONS AND CONCLUSIONS

Many light fragments are produced in high-energy nuclear fragmentation if the excitation and evaporation processes happen in the whole nucleus or spectator. Thus, the value of $\ln S_2$ will be low. If the excitation and evaporation process happen in the local region of the nucleus or spectator, the number of light fragments in the final state will be small. The value of $\ln S_2$ in the case of excluding the heaviest fragment will be low, too. This phenomenon can be reflected in the CMD rather than in the CMC [10,15]. In the correlation plane, this phenomenon is revealed in the region of low $\ln S_2$.

Some of light fragments with high or low temperatures are not excited but produced directly by a secondary collision in the nucleus or spectator. For a hot source, except direct fragments, we can consider most of light fragments as results of high excitation and evaporation processes. For a cold source, except heaviest fragment and direct fragments, most of light fragments are the results of low excitation and evaporation processes. Here we regard the nucleus or spectator as two local regions, the hot source, except direct fragments, and the cold source, except the heaviest fragment and direct fragments, in which the excitation and evaporation processes may be.

If the high excitation and evaporation processes happen in the whole nucleus or spectator, the number of light fragments in a typical event will be in the range from $Z/2$ to Z. The heaviest fragment will be helium. In such a case, an obvious difference between excluding and including the heaviest fragment will disappear due to small $d_{\max}$. If the excitation and evaporation processes happen in the local region of the nucleus or spectator, the number of light fragments in a typical events will be less than that of the former case. The heaviest fragment will be the residual nucleus, and it is generally greater than helium. In such a case, one will see an obvious difference between excluding and including the heaviest fragment due to great $d_{\max}$. Excluding the heaviest fragment, if the other fragments are H and He, the value of $\ln S_2$ will be in the range from 0 to $\ln 2$.

As a conclusion, in the case of excluding the heaviest fragment, we suggest that the conditional moment distribution or event distribution in the $\ln S_3$-$\ln S_2$ plane could be used in further studies. This work shows that the calculated results based on a two-source emission picture are in agreement with available experimental data. The MC simulated events can present the experimental data in the case of including and excluding the heaviest fragment, not only for the conditional moment correlation but also for the conditional moment distribution and the correlation between the heaviest fragment and the conditional moment.

ACKNOWLEDGMENTS

The authors would like to thank M.V. Tokarev and L.N. Barabash for their helpful comments. One of the authors (F.H.L.) gratefully acknowledges the support of the Laboratory of High Energies at the Joint Institute for Nuclear Research, Dubna, Russia. His work was also supported by the China State Education Department Foundation for Returned Overseas Scholars, Shanxi Provincial Foundation for Returned Overseas Scholars (Main Project), Shanxi Provincial Foundation for Leading Specialists in Science, and Shanxi Provincial Science Foundation for Young Specialists.

[1] J. Hüfner, Phys. Rep. **125**, 129 (1985).
[2] J. D. Bowman, Lawrence Berkeley Laboratory Report No. LBL 2908, 1973; J. Hüfner, GSI Report No. 80-1, 1980.
[3] H. R. Schmidt and J. Schukraft, Report No. CERN-PPE/92-42, 1992.
[4] X. Campi, J. Phys. A **19**, L917 (1986); X. Campi, Phys. Lett. B **208**, 351 (1988).
[5] H. E. Stanley, *Introduction to Phase Transition and Critical Phenomena* (Oxford University Press, Oxford, 1971).
[6] D. Stauffer, Phys. Rep. **54**, 1 (1979).
[7] C. J. Waddington and P. S. Freier, Phys. Rev. C **31**, 888 (1985).
[8] H. M. Liu, B. H. Sa, Y. M. Zheng, Z. D. Lu, and X. Z. Zhang, High Energy Phys. Nucl. Phys. **15**, 1053 (1991).
[9] F. H. Liu, Ph.D thesis, China Institute of Atomic Energy, Beijing, China, 1993.
[10] F. H. Liu and H. C. Sun, Can. J. Phys. **73**, 365 (1995), and references therein; F. H. Liu, Chin. J. Nucl. Phys. **17**, 200 (1995), and references therein.
[11] P. L. Jain, G. Singh, and A. Mukhopadhyay, Phys. Rev. C **50**, 1085 (1994); G. Singh and P. L. Jain, *ibid.* **49**, 3320 (1994); **54**, 3185 (1996).
[12] S. Y. Bahk, *et al.*, Phys. Rev. C **43**, 1410 (1991), and references therein.
[13] G. Singh, K. Sengupta, and P. L. Jain, Phys. Rev. C **41**, 999 (1990).
[14] A. Z. Mekjian, Phys. Rev. C **41**, 2103 (1990).
[15] F. H. Liu, Nuovo Cimento A **110**, 1361 (1997); F. H. Liu, Can. J. Phys. (to be published).
[16] F. H. Liu and Yu. A. Panebratsev (unpublished).